Frontiers in Bioscience Landmark

*Front. Biosci. (Landmark Ed)* **2023**; 28(3): 43
https://doi.org/10.31083/j.fbl2803043

*Original Research*

# Effects of Intestinal Microorganisms on Influenza-Infected Mice with Antibiotic-Induced Intestinal Dysbiosis, through the TLR7 Signaling Pathway

Jie Gao[1,†], Huifang Chen[2,3,†], Liuyue Xu[1], Shanglin Li[1], Huijun Yan[4], Lifang Jiang[4], Wenli Cheng[5,*], Zhenyou Jiang[1,*]

[1]Department of Microbiology and Immunology, Basic Medicine College, Jinan University, 510632 Guangzhou, Guangdong, China
[2]School of Chemistry & Pharmaceutical Sciences, Guangxi Normal University, 541001 Guilin, Guangxi, China
[3]School of Pharmacy, Guangdong Lingnan Institute of Technology, 510663 Guangzhou, Guangdong, China
[4]Key Laboratory of Tropical Disease Control (Sun Yat-Sen University), Ministry of Education, 510632 Guangzhou, Guangdong, China
[5]Department of Blood Transfusion, The Sixth Affiliated Hospital, Sun Yat-Sen University, 510632 Guangzhou, Guangdong, China
*Correspondence: chengwl@mail.sysu.edu.cn (Wenli Cheng); tjzhy@jnu.edu.cn (Zhenyou Jiang)
[†]These authors contributed equally.
Academic Editor: Rosa Alduina
Submitted: 14 September 2022 Revised: 7 December 2022 Accepted: 12 December 2022 Published: 2 March 2023

**Abstract**

**Background**: Stability of intestinal flora is not only important for maintaining stable immune functions; it is also a key immune channel communicating the interaction between lung and intestine. In this study, probiotics and fecal microbiota transplantation (FMT) were used to regulate influenza-infected mice with antibiotic-induced intestinal dysbiosis and the effects of intestinal microorganisms on these mice were subsequently observed and evaluated. **Methods**: Mice are housed in a normal environment with intranasal infection with influenza virus (FM1). Real-time quantitative polymerase chain reaction (RT-qPCR) was used to determine messenger RNA expression and lung viral replication of toll-like receptor 7 (TLR7), myeloid differentiation primary reaction 88 (MyD88) and nuclear factor $\kappa$B (ss) p65 in the TLR7 signaling pathway. Western blotting is used to measure the expression levels of TLR7, MyD88, and NF-$\kappa$B p65 proteins. Flow cytometry was used to detect the proportion of Th17/T regulated cells. **Results**: Results showed that compared with the simple virus group, both diversity and species of intestinal flora in influenza-infected mice with antibiotic-induced intestinal dysbiosis were lower, *in vivo* viral replication was significantly increased, lung and intestinal tissues were seriously damaged, degree of inflammation increased, expression of the TLR7 signaling pathway increased, and the Th1/Th2:Th17/Treg ratio decreased. Probiotics and FMT effectively regulated intestinal flora, improved pathological lung changes and inflammation caused by influenza infection, and adjusted the TLR7 signaling pathway and the Th1/Th2:Th17/Treg ratio. This effect was not obvious in TLR7$^{-/-}$ mice.In summary, by affecting the TLR7 signaling pathway, intestinal microorganisms reduced the inflammatory response in the lungs of influenza-infected mice with imbalances in antibiotic flora. **Conclusions**: By affecting the TLR7 signaling pathway, intestinal microorganisms reduced the inflammatory response in the lungs of influenza-infected mice with imbalances in antibiotic flora. In summary, damage to lung tissue and intestinal mucosa in influenza-infected mice with antibiotic-induced intestinal dysbiosis is more serious compared to simple virus-infected mice. Improving intestinal flora using probiotics or FMT can alleviate intestinal inflammation and improve pulmonary inflammation through the TLR7 signaling pathway.

**Keywords:** intestinal flora; probiotics; influenza A virus FM1 mouse lung adaptation strain; fecal microbiota transplantation; TLR7

## 1. Introduction

The complex relationship between intestinal flora and the human body spans various physiological activities and pathological processes, and consequently, is indispensable to the organism. The imbalance of the intestinal flora not only affects the functional state of the intestinal tract but also extensively influences the immune status and host function. Long-term antibiotic use can inhibit sensitive intestinal bacteria, allowing an excessive proliferation of drug-resistant bacteria, which is the primary reason for imbalances in intestinal flora [1]. Common methods for regulating imbalances in intestinal flora include the consumption of probiotics and fecal microbiota transplantation (FMT) from healthy donors [2]. Probiotics are active, beneficial microorganisms, commonly *Bifidobacterium* and *Lactobacillus*, colonizing the host and through the regulation of host mucosal and systemic immune functions or balancing of intestinal flora, promote nutrient absorption and maintenance of intestinal health. Therefore, promoting microorganisms or microbiota is beneficial to host health. FMT has been successfully used for the treatment of several diseases because FMT can regulate imbalances and restore homeostasis in the intestinal flora [3].

Influenza viruses belong to the Orthomyxoviridae family and can classified into the four following types: A, B, C, and D [4]. Influenza A viruses can easily cause an

influenza pandemic owing to antigenic variation [5]. Studies in antibiotic-treated mice have shown that mice with disorders of intestinal flora experience aggravated mucosal destruction, lymphoid tissue damage, disturbances in immune cell homeostasis, and changes in intestinal composition, and are susceptible to severe infectious and inflammatory disease outcomes [6].

Both the respiratory tract and the gastrointestinal tract belong to the mucosal immune system, have the same embryonic origin, and have similar structural similarities. Interactions between the intestine and the lung are mediated by microorganisms, metabolites, and free immune cells. Throughout the lung–intestinal axis, the intestinal flora remains stable, crucial to in maintaining the immune state and respiratory tract balance [7]. Recognition of microbial pathogens through pattern recognition receptors (PRRs) is required to initiate the natural immune response. PRRs recognize several conserved pathogenic molecules, or pathogen-associated molecular pattern (PAMP). As important PRRs, toll-like receptors (TLRs) can recognize pathogen molecules [8]. TLR7, highly expressed in human plasmacytoid dendritic cells [9], is a member of the TLR family that can recognizes single-stranded RNA viruses [10] including the influenza virus. After PAMP recognition, TLR7 recruits specific linker molecules that bind to Toll-IL-1 receptor (TIR) domains, including myeloid differentiation factor 88 (MyD88), and contain TIR structures, which can induce the interferon-$\beta$ linker molecule (TRIF), and subsequently, through a signaling cascade, eventually lead to the production of inflammatory factors, type I interferons, chemokines, and antibacterial peptides in these cells [11]. Finally, it induces nuclear transfer of NF-$\kappa$B and activates a signaling pathway eliciting an inflammatory response. However, whether the TLR7 signaling pathway in the innate immune system of the lung is related to the potential immune mechanisms of intestinal flora remains unclear.

In this study, we hypothesized that gut microbes could be used for treating antibiotic-induced intestinal dysbiotic influenza-infected mice through the TLR7 signaling pathway. To verify our hypothesis, we first established an animal model for influenza-infected mice with antibiotic-induced intestinal dysbiosis. After infecting with the influenza virus FM1 strain, these mice were treated with probiotics or FMT to restore intestinal flora. Finally, we assessed the effect of an imbalance in intestinal flora on the TLR7 signaling pathway in the lungs of influenza-infected mice. TLR7 signaling pathway was found to play an important role in reducing the inflammatory process in antibiotic-induced influenza-infected mice with intestinal dysbiosis.

## 2. Materials and Methods

### *2.1 Animals*

Animal experiments were performed with the approval and supervision of the Experimental Animal Ethics Committee of Jinan University (Guangdong, China). SPF-grade normal C57BL/6 wild-type mice were purchased from the Experimental Animal Center of Guangdong Province (production license SCXK [Guangdong] 2019-0056). Specific-pathogen-free (SPF), 6–8-week-old female C57BL/6J wild type (WT) mice, weighing 20 $\pm$ 2 g, and B6.129S1-*Tlr7* <tm1Flv>/J (*Tlr7*-/-) mice were purchased from China Guangdong Medical Experimental Animal Center and The Jackson Laboratory (Sacramento, CA, USA), respectively. All experimental mice were raised in an animal biosafety level 2 (ABSL-2) laboratory with a temperature-controlled animal feeding facility (temperature: 20 $\pm$ 2 °C; humidity: 50%), a 12-hour light cycle, and an independent ventilation cage (IVC). The endpoint of animal health is that the animal is moribund, or does not respond after being given a gentle stimulus; Dyspnea: typical symptoms are salivation and/or cyanosis of the nose and mouth; diarrhea or urinary incontinence; A clear sign of serious illness, at which point the animal is euthanized to avoid further unnecessary suffering. After placing the laboratory animals to be euthanized in the box, carbon dioxide is released to suffocate the experimental animals.

### *2.2 Groups*

Thirty WT and 30 *Tlr7*-/- mice were randomly divided into five groups: normal control (untreated), virus control (Virus), antibiotic treatment + virus (Model), model + probiotic recovery (Probiotics), and model + fecal microbiota transplantation (FMT). Model, Probiotics, and FMT groups were treated with antibiotics mixed in drinking water for 25 days. All mice were fed sterilized rat food. On day 26, feces from each group of mice were collected from their sterile containers; mice were then anesthetized using a 1% pentobarbital sodium intraperitoneal injection. The untreated group was treated with a 50 $\mu$L sterile saline nasal drip, while the other groups were infected with 50 $\mu$L of an influenza virus FM1 suspension. On day 27, the Probiotics group was treated with probiotics via intragastric administration for five days, while mice in the FMT group were transplanted with untreated mice feces for five consecutive days; other groups were fed normal saline for five days. On day 32, sacrifice mice by euthanasia. Each group of lungs, spleen, cecum, and feces were collected for analysis (Fig. 1a).

### *2.3 Antibiotics*

The antibiotic drinking water mix was prepared by adding ampicillin (1 mg/mL, Lot: 7918010110), neomycin (1mg/mL, Lot: 9311010150), metronidazole (1mg/mL, Lot: c10473109), gentamicin (0.5 mg/mL, Lot: H04J10Z89946), and vancomycin (0.5 mg/mL, Lot: H26M10Z84068) (all from Guangzhou Dingguo Biotechnology Co., Ltd., Guangzhou, China) to sterilized pure drinking water; this was replaced every three days.

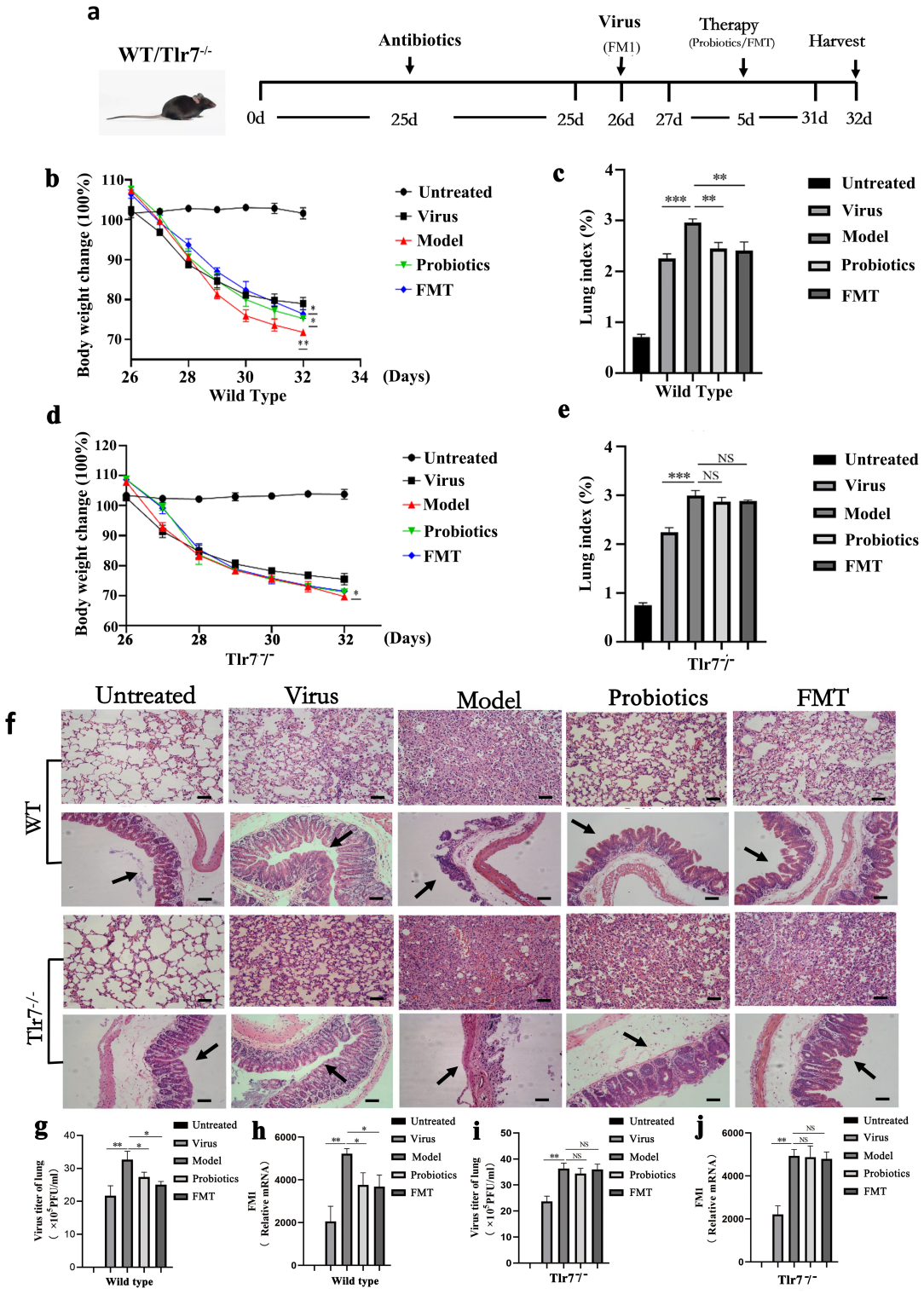


**Fig. 1. The changes of body weight and lung index, pathological analysis and virus replication were observed.** (a) is experimental flow graph. (b) and (c) represent changes to body weight and lung index, respectively, in each group of WT mice (n = 6). (d) and (e) represent changes to body weight and lung index, respectively, in *Tlr7*$^{-/-}$ mice of each group (n = 6). (f) represent pathological sections of lung and cecum tissues of WT mice and *Tlr7*$^{-/-}$ mice. Bars = 200 $\mu$m. The black arrow points to the mucosa of the cecum. (g) and (i) represent the titer of FM1 virus in the lung tissue of WT and *Tlr7-/-* mice on day 6 after infection (n = 6). (h) and (j) represent FM1 virus mRNA expression in the lung tissue of WT and *Tlr7-/-* mice on day 6 after infection (n = 6). *$p < 0.05$, **$p < 0.01$, ***$p < 0.001$, NS $p > 0.05$.

### 2.4 Probiotics

*Bifidobacterium and Lactobacillus* triple live bacteria tablets (Inner Mongolia Shuangqi Pharmaceutical Co., Ltd., Inner Mongolia,China , Chinese medicine S19980004) were used strictly according to the manufacturer's instructions; the daily dosage for each mouse was 0.78 g/kg. Probiotics were dissolved in sterilized saline and administered intragastrically at 0.2 mL/d [12,13].

### 2.5 Fecal Samples and 16S sRNA

Twenty-six days after antibiotic treatment, before being infected with virus, anus of each mouse was wiped with cotton swabs to stimulate defecation on a sterile container collecting feces. On day 32, following euthanasia, fecal samples were collected from the rectum of mice by opening the abdominal cavity using sterilized equipment in a biosafety cabinet. Collected feces were placed into sterile EP tubes and frozen at –80 °C. All procedures were completed within 30 min. The samples were sent to Guangdong Magigene technology Co., Ltd (Guangzhou, China) for testing.

The 16S rRNA gene was sequenced by Guangdong Magigene Biotechnology Co., Ltd (HiSeq2500/Miseq, PE250/PE300, Guangdong, China). Genomic DNA was extracted using the ALFA-SEQ Advanced Stool DNA Kit; the concentration and purity of DNA were detected using NanoDrop gel One. The hypervariable region of 16S rDNA V4–V5 was amplified using polymerase chain reaction (PCR), with barcode-tagged primers and TaKaRa Premix Taq® Version 2.0 (RR901A, TaKaRa, Guangzhou, China). Mixed PCR products were recovered using an E.Z.N.A.® Gel Extraction Kit (Omega, Nocross, Georgia, USA); target DNA fragments were recovered via elution with TE buffer. The Illumina Nova 6000 platform was used for PE250 sequencing of the expanded sublibrary. Head and tail primers were simultaneously removed using Cutadapt software, thus obtaining quality-controlled, paired-end clean reads. Fastp was used to tailor raw tag data with sliding window quality (– W4–M20), thus obtaining an effective splicing segment (clean tags). Clean tags of all samples were clustered (the similarity was 97% by default) to generate operational taxonomic units (OTUs); singleton OTUs and chimeras were simultaneously removed. To obtain annotated species information, each OTUs representative sequence was compared against SILVA (16s), RDP (16s), and Greengenes (16s) databases using usearch-sintax(version v11, San Francisco, USA).

### 2.6 FMT

Fresh feces from mice in the untreated group were collected and immediately re-suspended in aseptic saline; insoluble particles were filtered out. The filtrate was centrifuged at 4 °C for 15 min at 3000 × g, and the sediment collected. The sediment was dissolved in sterile saline to a final concentration of 400 mg/mL. Each mouse was treated with intragastric administration of 200 $\mu$L per day [14].

### 2.7 Virus

Influenza A virus (A/FM1/1/47) was provided by the Department of Immunology and Microbiology at the Jinan University and stored at –80 °C. After mice were anesthetized via intraperitoneal injection of 1% pentobarbital sodium, each was given 50 $\mu$L of virus solution for nasal infection.

### 2.8 Body Weight, Status and Lung Index of Mice

The status, coat color, vitality, drinking water, and survival status of mice in each group were observed daily. The body weight of each mouse was recorded at the same time each day, and the percentage of weight change was calculated according to the formula: percentage of weight change = (nth celestial body weight/day 0 body weight). Lung tissue sample was obtained and rinsed with aseptic phosphate buffer (PBS); the surface water was dried with filter paper before weighing. Lung index was calculated as (lung weight/body weight) × 100%.

### 2.9 Pathological Sections of Mice Lung and Cecum, Scoring Criteria

Lung tissue and cecum of mice were removed, fixed with 4% paraformaldehyde, embedded in paraffin, and sliced into 4 $\mu$m thick sections. Slices were dewaxed, dehydrated, and sealed following hematoxylin-eosin (HE) staining. Finally, histopathological images were observed and collected under a microscope. The histopathological lesion score of each mouse is presented as the average of the scores provided by the two pathologists. The scoring criteria were changed as previously described [15]. so that 0 indicates no lesions, 1–2 indicates mild inflammation with no necrosis, 3–6 indicates moderate inflammation with a high incidence of necrotic cells, and 7–9 indicates severe inflammation with frequent necrosis and edema.

### 2.10 Plaque Test to Detect Viral Titer

On day 6 after infection (day 32), lung tissue from mice was homogenized in 1 mL of Dulbecco's Modified Eagle's Medium (DMEM), and the supernatant obtained using centrifugation. Supernatant of lung tissue was diluted 10 times and to different concentrations. The Madin–Darby canine kidney (MDCK) cell plaque assay was used to determine viral titer in the supernatant of lung tissue. MDCK cells were cultured in a monolayer on a cell culture plate. Following full growth, after each well was washed with PBS, the supernatant of lung tissue with different dilution times was added to each well and incubated at 37 °C for 1 hr. A mixture of 2% carboxymethyl fiber and medium was added and incubated at 37 °C and 5% $CO_2$ for 4 days. The sample was fixed in 4% paraformaldehyde for 1 h, stained with crystal violet for 15 min, rinsed with pure water to remove excess dye, and the plaques counted. Plaque formation unit (PFU/mL) = (number of plaques per pore / inoculation per pore) × dilution [16].

**Table 1. Primers for RT-qPCR analysis.**

| Gene | Forward (5′ to 3′) | Reverse (5′ to 3′) |
|---|---|---|
| *Gapdh* | CTGAGCAAGAGAGGCCCTATCC | CTCCCTAGGCCCCTCCTGTT |
| *FM1* | GACCAATCCTGTCACCTCTGAC | AGGGCATTNTGGACAAAGCGTCTA |
| *Tlr7* | GGGTCCAAAGCCAATGTG | TGTTAGATTCTCCTTCGTGATG |
| *MyD88* | CGATTATCTACAGAGCAAGGAATG | ATAGTGATGAACCGCAGGATAC |
| *NF-κB p65* | ATTCTGACCTTGCCTATCTAC | TCCAGTCTCCGAGTGAAG |

### *2.11 Quantitative Reverse Transcription (RT-qPCR)*

Total RNA was extracted from lung tissue homogenate using RNAiso plus (Takara, Kusatsu, Japan). After testing RNA quality, the PrimeScriptTM RT kit and SYBR Green PCR Master Mix (Takara, Kusatsu, Japan) were used for cDNA synthesis and qPCR detection. Reverse transcription was performed in a Bio-Rad S1000 thermal cycler (Bio-Rad, Berkeley, CA, USA). qPCR was performed using the CFX Connect real-time PCR detection system (Bio-Rad, Berkeley, CA, USA). Experimental procedures were as follows: 95 °C, 30 s, 5 s, 60 °C, 30 s, cycle 40 amplification cycles, 95 °C, 10s. All primers (Table 1) were designed and synthesized by Shanghai Shenggong Bioengineering Co., Ltd (Guangzhou, China). All samples were equipped with 3 multiple holes, and the experiment was repeated three times. GAPDH was used as the internal reference and expression was calculated using the cycle threshold method ($2^{-\Delta\Delta Ct}$) [17].

### *2.12 Flow Cytometry*

Mice spleen tissues were washed and homogenized in 1640 medium without serum. Peripheral blood mononuclear cells (PBMCs) were collected using a mouse lymphocyte separation solution (Multi Sciences, Hangzhou, China), according to the manufacturer's instructions. PBMCs were then suspended in 1640 culture containing 10% fetal bovine serum (FBS), and the cell concentration adjusted to $1 \times 10^6$/mL. In order to detect Th1, Th2, and Th17 cells, phorbol 12-myristate 13-acetate (0.05 $\mu$g/mL, PMA), ionomycin (1 $\mu$g/mL), brefeldin A (3 $\mu$g/mL, BFA), and monensin (1.4 $\mu$g/mL) were added according to stimulant and blocker reagent instructions (both purchased from Multi Sciences, Hangzhou, China), and incubated at 37 °C for 5 h in a 5% $CO_2$ atmosphere. Cells were labeled with anti-CD4, interferon (IFN)-g, interleukin (IL)-4, and IL-17A antibodies. In order to detect T regulatory cells (Treg) cells, anti-CD4 and CD25 antibodies were added and incubated at 4 °C for 30 min; cells were re-suspended in a membrane-breaking solution (fixation/permeabilization concentrate: fixation/permeabilization diluent = 1:3, eBioscience, USA) and incubated at 4 °C for 30 min. After washing with 1X permeabilization buffer (eBioscience, USA), anti-Foxp3 antibody was added and incubated for 30 min at 4 °C without light. Th1, Th2, Th17, and Treg cells were defined as CD4 + IFN-g +, CD4 + IL-4 +, CD4 + IL-17A +, and CD4 + CD25 + Forxp3 + T cells, respectively (All antibodies information was in Table 2). All stained cells were detected using flow cytometry FACS VERSE (Becton Dickinson Biosciences, Franklin Lake, NJ, USA), and the results analyzed using FlowJo v10 (FlowJo, Ashland, OR, USA).

**Table 2. Antibodies for flow cytometry analysis.**

| Antibody | Labels used | Company |
|---|---|---|
| CD4 | FITC | eBioscience |
| IFN-$\gamma$ | APC | eBioscience |
| IL-4 | PE | eBioscience |
| IL-17A | PE-cyanine7 | eBioscience |
| CD25 | APC | eBioscience |
| Foxp3 | PE | eBioscience |

### *2.13 Western Blotting for Tlr7, MyD88, and NF-κB p65*

Mouse lung tissue was extracted using RIPA lysis buffer (LOT: 6171803, Multi Sciences, Hangzhou, China), with total protein extracted after homogenization. Total protein was quantified using a BCA protein quantitative kit (LOT: A91041, Multi Sciences, Hangzhou, China). Protein was separated using 10% sodium dodecyl sulfate-polyacrylamide gel electrophoresis (SDS-PAGE) and transferred to a polyvinylidene fluoride membrane (PVDF) membrane sealed with 5% skim milk powder. The membrane was then incubated with rabbit anti-mouse monoclonal antibodies against RIG-I (CST, 4200S, 1:1000), MA VS (CST, 4983S, 1:1000), NF-$\kappa$B p65 (CST, 8242S, 1:1000), and GADPH (CST, 2118S, 1:1000) at 4°C. Cells were then incubated with horseradish peroxidase-labeled goat anti-rabbit IgG (LOT: A91053, Multi Sciences, Hangzhou, China). Protein bands were detected using an electrochemiluminescence (ECL) kit (LOT: A90844, MultiSciences, Hangzhou, China), and analyzed using ImageJ software (v1.8.0.112, NIH, Bethesda, USA).

### *2.14 Statistical Analysis*

Statistical analysis was performed using GraphPad Prism 8.0 software (Beijing, China). Results were expressed as mean $\pm$ standard deviation (SD). Two-way analysis of variance (ANOVA) followed by Tukey's multiple comparison tests was executed. A $p$ value of $<0.05$ was regarded as statistically significant.

## 3. Results

### *3.1 Changes in WT and Tlr7$^{-/-}$ Mice Following Antibiotic Treatment*

#### Changes in Intestinal Flora of WT and Tlr7$^{-/-}$ Mice Treated with Mixed Antibiotics

The Venn diagram for Operational Taxonomic Units (OTU) shows the number of common and endemic species between different groups. Total OTUs for WT and *Tlr7*$^{-/-}$ mice treated with antibiotics were 410 and 308, respectively, which was; significantly lower compared to the untreated group, at 1381 and 1151, respectively. Common OTUs were 372 and 294, with a few OTUs differ in the untreated group (Sup.S1a, S1b). A microbial community composition columnar analysis was performed and the composition of the microbial community at the family level was analyzed. In the untreated group of WT mice, *Muribaculaceae* (0.437) was the dominant flora, and *Lachnospiraceae* (0.150) and *Prevotellaceae* (0.080) were common, accounting for a certain proportion. In antibiotic-treated WT mice, flora composition changed diamatically. *Enterobacteriaceae* (0.840) was the most dominant, while *Clostridiaceae* (0.116) constituted a small proportion; the abundance of other bacteria showed extreme reduction (Sup.S1c). The untreated group of *Tlr7*$^{-/-}$ mice showed results similar to untreated group of the WT mice, with *Muribaculaceae* (0.527) being the dominant group, and other bacteria, including *Lachnospiraceae* (0.145) and *Prevotellaceae* (0.097), accounted for a certain proportion. jie of *Tlr7*$^{-/-}$ mices, in addition to a large increase in *Enterobacteriaceae* (0.321) and *Bacteroidaceae* (0.074), the abundances of *Tannerellaceae* (0.514) and *Akkermansiaceae* (0.065) also increased significantly, while those of other families decreased significantly (Sup.S1d). Results of the Venn diagram and community composition columnar analysis showed that the abundance of intestinal microflora changed significantly following antibiotic treatment, resulting in mice showing flora imbalance.

### *3.2 Changes in FM1 Influenza-Infected Mice with Antibiotic-Induced Intestinal Dysbiosis*

#### 3.2.1 Changes in Body Weight and Lung Indexes

Following the FM1 influenza virus infection, the body weight of mice decreased significantly, and they experienced loss of appetite, fluffy and rough hair, and decreased activity. Six days after infection, weight loss in the WT Model group was more severe than in the WT Virus group ($p < 0.01$), whereas body weight in the Probiotics and FMT groups improved slightly (Fig. 1b). The lung indexes of the WT Model group was 2.96, significantly higher than 2.25 in the Virus group ($p < 0.001$). The lung indexes of the WT Probiotics and FMT groups were lower than in the Model group, suggesting more serious inflammation in the Model group, which was alleviated in the Probiotics and FMT groups (Fig. 1c). Body weights in the *Tlr7*$^{-/-}$ Model group were significantly different from the Virus group ($p < 0.05$), while Probiotics and FMT groups showed no significant difference compared to the Model group (Fig. 1d) with similar lung indexes (Fig. 1e). These results indicated that probiotic use and FMT could alleviate weight loss and lung indexes in WT mice but had no significant effect on *Tlr7*$^{-/-}$ mice.

#### 3.2.2 Histopathological Analysis and Viral Replication

Microscopic observation showed that alveoli structure in the untreated group of WT and *Tlr7*$^{-/-}$ mice was regular and intact, with no inflammatory secretion in the alveolar cavity or cellular infiltration in the alveolar interstitium (Fig. 1f). Mucosal structure of the cecum was intact; epithelial monolayer columnar cells were neatly arranged; colorectal glands were evenly distributed, and solitary lymphoid nodules were seen in the lamina propria (Fig. 1f). Compared to the untreated group, obvious inflammation injury, destruction of alveolar structure, thickening of alveolar diaphragm, alveolar interstitial edema, and lymphocyte infiltration were observed in WT and *Tlr7*$^{-/-}$ mice of the Virus group (Fig. 1f). In the cecum, the number of large, irregularly distributed intestinal glands increased, as also the lymphocytes in the lamina propria; however, the overall mucosal structure was intact (Fig. 1f). Compared to the Virus group, inflammation injury to the lung tissue in the Model group of WT and *Tlr7*$^{-/-}$ mice was more serious, with large structural alveolar damage, alveolar diaphragm thickening, interstitial edema, some tissue necrosis and exfoliation formed cavities, and high lymphocyte infiltration (Fig. 1f). The mucosal layer of the cecum was seriously damaged; the number of epithelial monolayer columnar cells decreased; colorectal glands were ruptured and necrotized, and high lymphocytes infiltration of lymphocytes occurred (Fig. 1f). After infection, cecal tissue injury in WT mice treated with probiotics and FMT was lesser relative to the the Model group; exfoliation of epithelial monolayer columnar cells reduced significantly, and the colorectal glands were partly intact (Fig. 1f). Compared to the Model group, inflammation injury to the lung tissue reduced slightly, along with the infiltration of inflammatory cells, and the alveolar septum was thinner (Fig. 1f). In *Tlr7*$^{-/-}$ mice, mucosal damage to the cecal tissue in infected animals treated with probiotics and FMT was slightly lower compared to the Model group (Fig. 1f); however, no significant differences in the degree of inflammation injury to the lung tissue between the Model and Probiotic groups were observed (Fig. 1f). No viral titer or FM1 mRNA expression was detected in WT or *Tlr7*$^{-/-}$ mice in the untreated group. In WT mice, viral titer and FM1 mRNA levels in the Model group were significantly higher compared to the Virus group. Viral titer and FM1 mRNA expression in Probiotics and FMT groups were lower relative to the Model group (Fig. 1g,h). In *Tlr7*$^{-/-}$ mice, viral titer and FM1 mRNA expression in the Model group were significantly higher compared to the Virus group; however, no

significant differences in viral titer and FM1 mRNA expression in mice treated with probiotics and FMT compared to the Model group were observed (Fig. 1i,j). To further evaluate the protective effect of Probiotics and FMT on pulmonary inflammation in influenza-infected mice, a double-blinded experiment, as described in Section 2.9, was performed to systematically assess the severity of lung pathology in mice. After probiotic administration and FMT treatment, the inflammatory response of lung tissues in WT mice reduced significantly (Sup.S2a). Notably, compared to the model control, histopathological section staining and histological scoring results showed that probiotic and FMT treatment caused milder inflammatory reactions in the lung tissues of the WT mice. However, after treatment with probiotics and FMT, the inflammatory responses of lung tissues of *Tlr7*$^{-/-}$ mice showed no significant improvment compared to the model group (Sup. S2b). Histopathological section staining and histological scoring results showed that probiotic and FMT treatment could not alleviate lung tissue inflammation in*Tlr7*$^{-/-}$ mice. These results suggest that probiotics and FMT could regulate the intestinal flora of WT mice, and reduce viral replication in WT lung tissue but had no significant effect on the lung tissue of *Tlr7*$^{-/-}$ mice.

### 3.2.3 Changes in Intestinal Flora

Intestinal microflora in mice of each group was analyzed 16S sequencing analysis, $\alpha$-diversity index, and community composition columnar analysis. Shannon's and Simpson's diversity indices reflected the richness and evenness of species, respectively. Results indicated no significant differences in Shannon's and Simpson's indices between the untreated and Virus groups of WT mice. Shannon's and Simpson's indices were significantly lower and higher, respectively, in the Model group compared to the Virus group. Shannon's index in mice treated with probiotics and FMT was higher, while Simpson's index was lower compared to the Model group (Sup.S3a, S3b). In *Tlr7*$^{-/-}$ mice, results of the $\alpha$-diversity index were similar to those for the WT mice, with the lowest and highest Shannon's and Simpson's indices, respectively, in the Model group, and a dramatic reduction in the Probiotic and FMT groups (Sup.S3c, S3d). At the family level,the microbial community composition columnar analysis chart depicted that the WT untreated group had the highest *Muribaculaceae* (0.405) relative abundance, followed by Lachnospiraceae (0.216) and Ruminococcaceae (0.078), belonging to the same phylum of thick-walled bacteria as Lachnospiraceae. The proportion of species in the Virus group changed, with major alterations in *Bacteroidaceae* (0.198), *Muribaculaceae* (0.192), and *Akkermansiaceae* (0.141). The proportion of *Lachnospiraceae* (0.087) decreased but that of *Enterobacteriaceae* (0.053) increased. In the Model group, *Enterobacteriaceae* (0.734) was dominant, whereas *Akkermansiaceae* (0.199), *Muribaculaceae* (0.001), and other species were substantially suppressed. With probiotic and FMT treatment, *Enterobacteriaceae* (0.327 and 0.241, respectively) decreased, while *Bacteroidaceae* (0.161 and 0.228, respectively) increased; other species showed signs of recovery. In the FMT group, the proportion of *Muribaculaceae* (0.088) increased significantly (Sup.S3e). In the untreated group comprising *Tlr7*$^{-/-}$ mice, *Muribaculaceae* (0.528) was dominant, followed by *Lachnospiraceae* (0.151) and *Prevotellaceae* (0.095). In the Virus group, the abundance of *Bacteroidaceae* (0.301) was higher than that of *Muribaculaceae* (0.239), and *Enterobacteriaceae* (0.107) increased significantly. Proportions of species in the Model group changed most prominently, with *Tannerellaceae* (0.546) and *Enterobacteriaceae* (0.404) showing an increase, while *Muribaculaceae* (0.003) decreased significantly. Following intragastric administration of probiotics and FMT, Tannerellaceae (0.422 & 0.047) and Enterobacteriaceae (0.377 & 0.181) decreased, while *Bacteroidaceae* (0.470) increased significantly only in the FMT group (Sup.S3f). These results suggest that probiotics use and FMT adjusted imbalances in the intestinal flora of mice.

### 3.2.4 mRNA and Protein Expressions of TLR7, MyD88, and NF-$\kappa$B p65

To further verify the relationship between intestinal flora and the TLR signaling pathway, we analyzed the expressions of TLR7 and downstream MyD88 NF and NF-$\kappa$B p65. In WT mice, relative mRNA expressions of TLR7, MyD88, and NF-$\kappa$B p65 in the Virus group were higher than in the untreated group. Key factors of the TLR7 signaling pathway in the Model group were significantly higher relative to the Virus group. Relative mRNA expressions of TLR7, MyD88, and NF-$\kappa$B p65 in the probiotic and FMT groups reduced significantly relative to the Model group (Fig. 2a). In *Tlr7*$^{-/-}$ mice, no significant change in key factors of the TLR7 signaling pathway in the lungs of probiotic and FMT-treated mice (Fig. 2b). In WT mice, protein expressions of TLR7, MyD88, and NF-$\kappa$B p65 in the lung tissues of the Virus group were higher relative to the untreated group but were the highest in the Model group. All three proteins were downregulated in the Probiotics and FMT groups (Fig. 2c,d). In *Tlr7*$^{-/-}$ mice, protein expressions in the Model group were significantly higher relative to the Virus group; however, there was no significant difference in expression between the Model, Probiotics, and FMT groups (Fig. 2c,d).

### 3.2.5 Changes in Th1/Th2 and Th17/Treg in the Spleen Tissues of Mice

To further assess inflammation in mice, Th1/Th2 and Th17/Treg were detected in the spleen tissues of mice by flow cytometry (Fig. 3a). In WT mice, the balance between Th1/Th2 and Th17/Treg in the Model group was significantly disrupted (Fig. 3b,c); however, the ratio was differ-

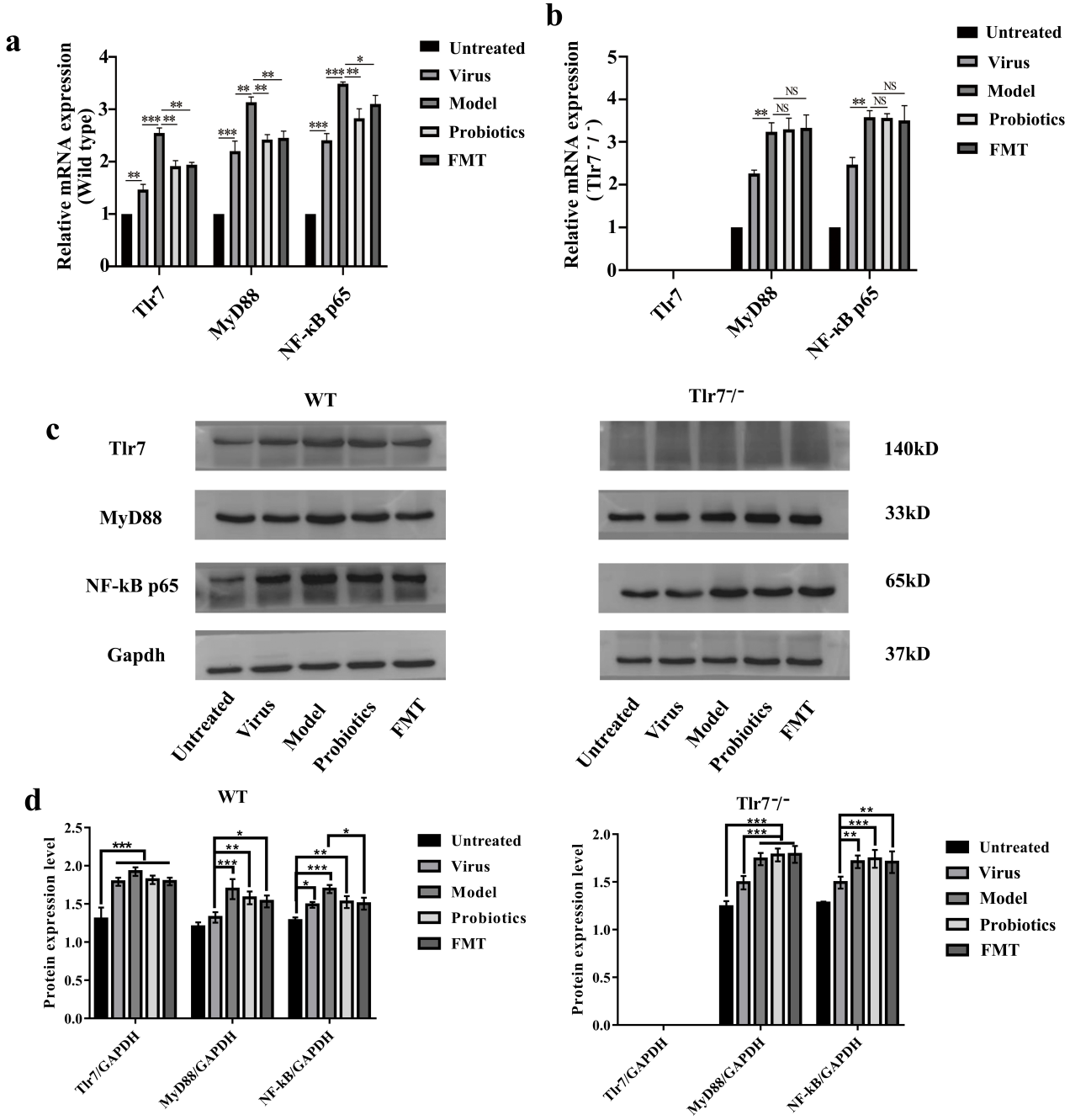


**Fig. 2. mRNA and proteins expressions of TLR7, MyD88, and NF-κB p65.** (a) and (b) Relative mRNA expression of TLR7, MyD88, and NF-κB p65 in the lung tissue of WT mice and *Tlr7*$^{-/-}$ mice. (c) Western blotting results of Tlr7, MyD88, and NF-κB p65 protein expression in the lungs of WT and *Tlr7*$^{-/-}$ mice. n = 6, (d) is the quantitative analysis of WB in the (c). *$p < 0.05$, **$p < 0.01$, ***$p < 0.001$, NS $p > 0.05$.

ent compared to the Virus group, showing a decrease when bacteria were destroyed using mixed antibiotics (Fig. 3b, c). The ratio in the Probiotics and FMT groups was significantly adjusted relative to the Model group (Fig. 3b,c). However, in *Tlr7*$^{-/-}$ mice, results in Probiotics and FMT groups were not significantly different compared to the Model group, whereby the balance between Th1/Th2 and Th17/Treg remained seriously disrupted (Fig. 3b,c).

## 4. Discussion

In this study, we focused on the important effects of regulation of intestinal flora through the TLR7 signaling pathway in influenza-infected mice with antibiotic-induced intestinal dysbiosis. Inflammation of the lungs and intestines in *Tlr7*$^{-/-}$ mice was more severe than in influenza-infected mice without antibiotic administration. Although probiotics and FMT improved the severity of lung and in-

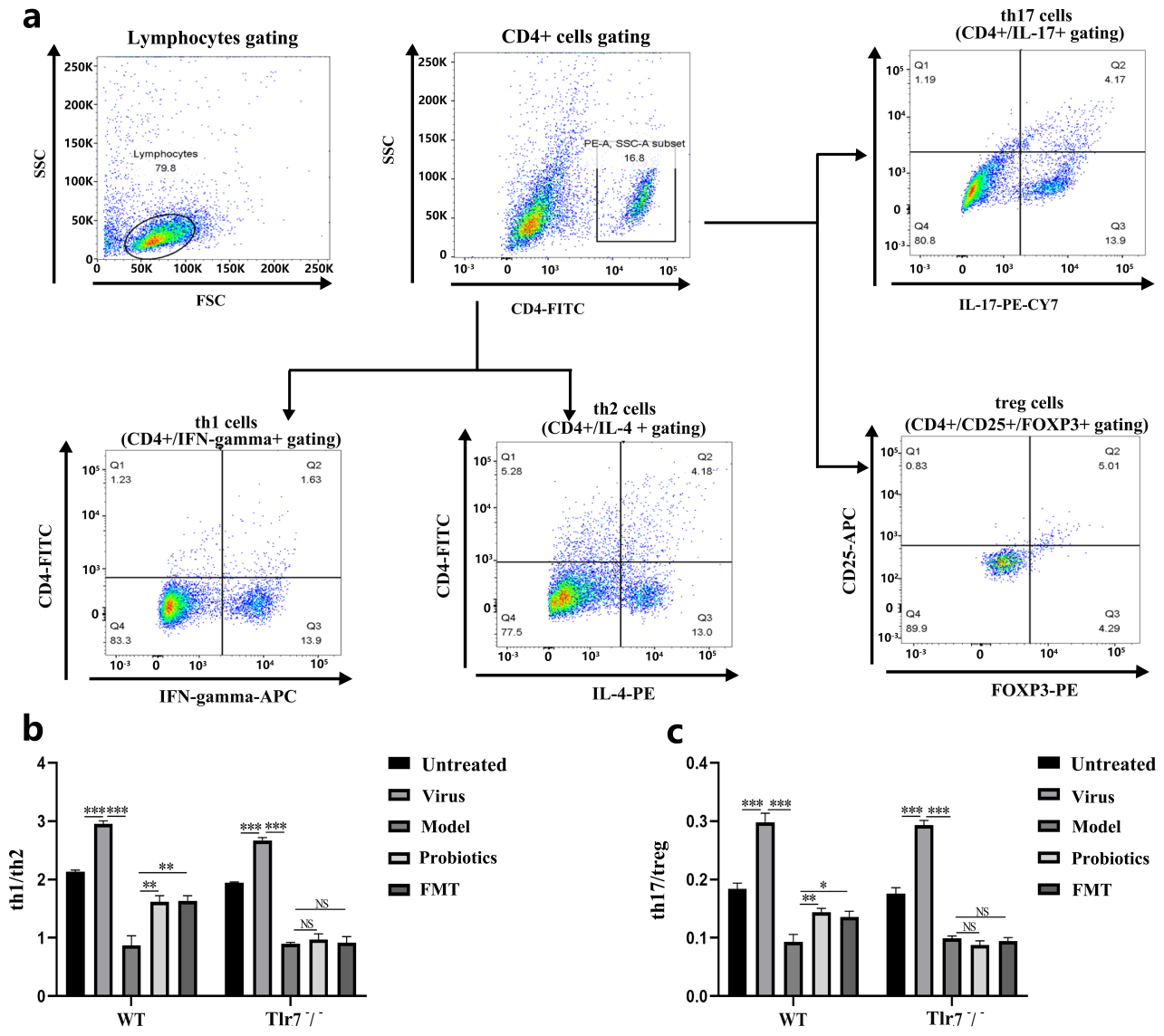


**Fig. 3. Results of Th1/Th2 and Th17/Treg in mice.** (a) Th1, Th2, Th17, and Treg cells were analyzed using flow cytometry. (b) Results of Th1/Th2 in WT and *TLR7*$^{-/-}$ mice. (c) Results of Th17/Treg in WT and *Tlr7*$^{-/-}$ mice. n = 6, *$p < 0.05$, ** $p < 0.01$, ***$p < 0.001$, NS $p > 0.05$.

testinal infection in WT mice, these had no significant effect on pulmonary infection in *Tlr7*$^{-/-}$ mice.

First, it was necessary to establish an influenza mouse model with antibiotic-induced intestinal dysbiosis. Under normal conditions, the intestinal flora is in a dynamic balance, with rich and diverse species showing relatively stable proportions. The four main phyla—Firmicutes Bacteroidetes Actinobacteria and Proteobacteria account for more than 90% of total intestinal bacteria [18,19]. Many factors can cause an imbalance in the intestinal flora, including environmental, nutritional, drug use, and antibiotic abuse [20]. In this study, five different antibiotics were administered to mice for destroying the intestinal flora, resulting in serious damage to species abundance [21,22]. Mice were infected with the FM1 influenza virus to establish an influenza-infected mouse model with antibiotic-induced intestinal dysbiosis and probiotics and FMT were used to regulate and rebuild intestinal microbial balance and prevent diseases. Common probiotics include Lactobacillus, Bifidobacterium, Streptococcus, Escherichia, and Bacillus [23]. The Bifidobacterium and Lactobacillus triple live bacteria tablets used in this study are common probiotic preparations comprising *B. longum*, *L. bulgaricus*, and *S. thermophilus*. FMT is also an effective method to restore and regulate destroyed intestinal flora, often playing an important role in many diseases, including diabetes, liver cirrhosis, and *Clostridium difficile* infections [24].

McDermott and others propose that mucosal immune cells distributed across the body can interact with different mucosal tissues and organs [25]. In the Virus group,

infection with the influenza virus in the lungs led to intestinal inflammatory cell infiltration. After the regulation of intestinal flora in the Probiotics and FMT groups, lung tissues followed the recovery trend of the intestinal mucosa, to alleviate inflammation associated with viral infections. A study by Takeshi Ichinohe reported that balanced intestinal flora could regulate respiratory mucosal immunity through the activation of inflammatory bodies, thus potentially regulating the respiratory mucosa via PRRs and releasing interleukin along with Treg cells regulation [26]. Furthermore, probiotics or FMT repaired intestinal flora and improved intestinal mucosa in *Tlr7*$^{-/-}$ mice; however, there was no significant effect on lung tissue and viral replication. This suggested that the TLR7 signaling pathway underlies intestinal flora regulation of pulmonary inflammation in influenza-infected mice with antibiotic-induced intestinal dysbiosis.

TLR7 recognizes the ssRNA genome of the influenza viruses, which acts by activating MyD88, inducing NF-$\kappa$B p65 activation, cytokine secretion, and inflammatory responses [27]. Previous reports indicate that the TLR/NF-$\kappa$B signal is overexpressed in mice with consumed intestinal flora, whereas the innate immune responses and intestinal flora recovery play an important role in defending against pathogens, and maintaining the dynamic balance of the immune system and intestinal microflora [28]. We verified that intestinal flora regulation mediated injury of the intestinal mucosa in *Tlr7*$^{-/-}$ mice; however, no significant effect was observed on lung tissues. This further suggested that the TLR7/NF-$\kappa$B signaling pathway was required for intestinal flora regulation on lung tissue.

According to phenotypic and functional characteristics, CD4+ T cells can be classified as Th1, Th2, Th17, Th22, T follicular helper cells (TfH), and Treg. The ratio of Th1/lr7$^{-/-}$ Th2:Th17/Treg plays an important role in hypersensitivity and autoimmune diseases [29,30]. Disrupting the balance of intestinal flora with antibiotics resulted in decreased IFN-g and IL-17 expressions, an increased proportion of CD4+ CD25+ Foxp3+ Treg cells, and a decreased ratio of Th1/Th2:Th17/Treg, unlike the increasing trends during simple virus infections [31,32]. Hence, compared to simple virus-infected mice, Th1/Th2 and Th17/Treg cells in influenza-infected mice following intestinal dysbiosis were greatly imbalanced. The same experiment on *Tlr*$^{-/-}$ mice showed that following probiotic administration or FMT, although intestinal flora and mucosa recovered, the ratio of Th1/Th2:Th17/Treg remained consistenely low. TLR7 not only participates in the development of airway inflammation, further activating MyD88 and NF-$\kappa$B signaling pathways but also promotes the transdifferentiation of CD4+ T cells into Tregs [33]. Therefore, the TLR7/ NF-$\kappa$B signaling pathway can regulate the balance of Th1 and Th2 cells through Treg cells regulations.

## 5. Conclusions

In summary, damage to lung tissue and intestinal mucosa in influenza-infected mice with antibiotic-induced intestinal dysbiosis is more serious compared to simple virus-infected mice. Improving intestinal flora using probiotics or FMT can alleviate intestinal inflammation and improve pulmonary inflammation through the TLR7 signaling pathway. Therefore, further understanding of the relationship between the molecular mechanism underlying the TLR7 signaling pathway and lung and intestinal mucosa may provide a new strategy for the development of antiviral therapy.

## Availability of Data and Materials

The data and material for the current study are available from the corresponding author upon reasonable request.

## Author Contributions

Conceptualization—JG, HC, LX, SL, HY, LJ, WC, ZJ. Data curation—JG, HC, LX, SL. Funding acquisition—ZJ. Investigation—JG, HY, LJ. Methodology—LX, SL, HY, LJ, WC. Software—JG and SL. Visualization—JG and HC. Writing – original draft—JG. Writing – review & editing—JG, HC, LX, SL, HY, LJ, WC, ZJ. All authors contributed to editorial changes in the manuscript. All authors read and approved the final manuscript.

## Ethics Approval and Consent to Participate

This study was approved by the Experimental Animal Ethics Committee of Jinan University (Guangzhou, China) (Approval No. IACUC-20191120-06).


## Acknowledgment

Not applicable.

## Funding

This study was financially supported by the Science and Technology Projects of Guangdong Province (2019A1515011071), the National Natural Science Foundation of China (no. 82074133), National Science and Technology Major Infectious Diseases Project during the 12th 5-Year Plan Period (2014ZX10003002-003–002). The Fundamental Research Funds for the Central Universities (NO: 21621101).


## Conflict of Interest

The authors declare no conflict of interest.

## References


[1] Ekmekciu I, von Klitzing E, Neumann C, Bacher P, Scheffold A, Bereswill S, *et al*. Fecal Microbiota Transplantation, Commensal *Escherichia coli* and *Lactobacillus johnsonii* Strains Differentially Restore Intestinal and Systemic Adaptive Immune

Cell Populations Following Broad-spectrum Antibiotic Treatment. Frontiers in Microbiology. 2017; 8: 2430.
[2] Ekmekciu I, von Klitzing E, Fiebiger U, Escher U, Neumann C, Bacher P, *et al*. Immune Responses to Broad-Spectrum Antibiotic Treatment and Fecal Microbiota Transplantation in Mice. Frontiers in Immunology. 2017; 8: 397.
[3] Wang Z, Yang Y, Chen Y, Yuan J, Sun G, Peng L. Intestinal microbiota pathogenesis and fecal microbiota transplantation for inflammatory bowel disease. World Journal of Gastroenterology. 2014; 20: 14805–14820.
[4] Krammer F. Emerging influenza viruses and the prospect of a universal influenza virus vaccine. Biotechnology Journal. 2015; 10: 690–701.
[5] Rewar S, Mirdha D, Rewar P. Treatment and Prevention of Pandemic H1N1 Influenza. Annals of Global Health. 2015; 81: 645–653.
[6] Chen C, Wu G, Kuo R, Shih S. Role of the intestinal microbiota in the immunomodulation of influenza virus infection. Microbes and Infection. 2017; 19: 570–579.
[7] Shi N, Li N, Duan X, Niu H. Interaction between the gut microbiome and mucosal immune system. Military Medical Research. 2017; 4: 14.
[8] Janeway CA. Approaching the asymptote? Evolution and revolution in immunology. Cold Spring Harbor Symposia on Quantitative Biology. 1989; 54: 1–13.
[9] Reizis B, Bunin A, Ghosh HS, Lewis KL, Sisirak V. Plasmacytoid dendritic cells: recent progress and open questions. Annual Review of Immunology. 2011; 29: 163–183.
[10] Akira S, Uematsu S, Takeuchi O. Pathogen recognition and innate immunity. Cell. 2006; 124: 783–801.
[11] Kawai T, Akira S. The role of pattern-recognition receptors in innate immunity: update on Toll-like receptors. Nature Immunology. 2010; 11: 373–384.
[12] Wang Y, Gao Y, Feng J, Dou Y. Effect of Modified Xijiao Dihuang Decoction on Intestinal Flora and Th17/Treg in Rats with Radiation Enteritis. Chinese Journal of Integrative Medicine. 2020; 27: 198–205.
[13] Jia L, Zhang M. Comparison of probiotics and lactulose in the treatment of minimal hepatic encephalopathy in rats. World Journal of Gastroenterology. 2005; 11: 908–911.
[14] Wei Y, Chen Y, Gong H, Li N, Wu K, Hu W, *et al*. Fecal Microbiota Transplantation Ameliorates Experimentally Induced Colitis in Mice by Upregulating AhR. Frontiers in Microbiology. 2018; 9: 1921.
[15] Belser JA, Wadford DA, Pappas C, Gustin KM, Maines TR, Pearce MB, *et al*. Pathogenesis of pandemic influenza A (H1N1) and triple-reassortant swine influenza A (H1) viruses in mice. Journal of Virology. 2010; 84: 4194–4203.
[16] Yan Y, Fu Y, Wu S, Qin H, Zhen X, Song B, *et al*. Anti-influenza activity of berberine improves prognosis by reducing viral replication in mice. Phytotherapy Research. 2018; 32: 2560–2567.
[17] Fu Y, Yan Y, Qin H, Wu S, Shi S, Zheng X, *et al*. Effects of different principles of Traditional Chinese Medicine treatment on TLR7/NF-κB signaling pathway in influenza virus infected mice. Chinese Medicine. 2018; 13: 42.
[18] Walter J, Ley R. The human gut microbiome: ecology and recent evolutionary changes. Annual Review of Microbiology. 2011; 65: 411–429.
[19] Becattini S, Taur Y, Pamer EG. Antibiotic-Induced Changes in the Intestinal Microbiota and Disease. Trends in Molecular Medicine. 2016; 22: 458–478.
[20] Biedermann L, Rogler G. The intestinal microbiota: its role in health and disease. European Journal of Pediatrics. 2015; 174: 151–167.
[21] Abt MC, Osborne LC, Monticelli LA, Doering TA, Alenghat T, Sonnenberg GF, *et al*. Commensal bacteria calibrate the activation threshold of innate antiviral immunity. Immunity. 2012; 37: 158–170.
[22] Lagkouvardos I, Lesker TR, Hitch TCA, Gálvez EJC, Smit N, Neuhaus K, *et al*. Sequence and cultivation study of Muribaculaceae reveals novel species, host preference, and functional potential of this yet undescribed family. Microbiome. 2019; 7: 28.
[23] Gupta V, Garg R. Probiotics. Indian Journal of Medical Microbiology. 2009; 27: 202–209.
[24] Zhang F, Cui B, He X, Nie Y, Wu K, Fan D, *et al*. Microbiota transplantation: concept, methodology and strategy for its modernization. Protein & Cell. 2018; 9: 462–473.
[25] McDermott MR, Clark DA, Bienenstock J. Evidence for a common mucosal immunologic system. II. Influence of the estrous cycle on B immunoblast migration into genital and intestinal tissues. Journal of Immunology (Baltimore, Md.: 1950). 1980; 124: 2536–2539.
[26] Ichinohe T, Pang IK, Kumamoto Y, Peaper DR, Ho JH, Murray TS, *et al*. Microbiota regulates immune defense against respiratory tract influenza A virus infection. Proceedings of the National Academy of Sciences of the United States of America. 2011; 108: 5354–5359.
[27] Arora S, Ahmad S, Irshad R, Goyal Y, Rafat S, Siddiqui N, *et al*. TLRs in pulmonary diseases. Life Sciences. 2019; 233: 116671.
[28] Fu W, Zhao J, Liu X, Gao Y, Zheng C. The roles of the TLR/NF κB signaling pathway in the mutual interactions between the lung and the large intestine. Molecular Medicine Reports. 2018; 18: 1387–1394.
[29] Zhang H, Zheng X, Zhu J. Th1/Th2/Th17/Treg cytokines in Guillain-Barré syndrome and experimental autoimmune neuritis. Cytokine & Growth Factor Reviews. 2013; 24: 443–453.
[30] Tong J, Hu X, Cai W, Dai X, Wang L. Puerarin alleviates delayed-type hypersensitivity via cytokine inhibition by modulating Th1/Th2 balance. Experimental and Therapeutic Medicine. 2018; 15: 4441–4447.
[31] Misra RS. A Review of the CD4+ T Cell Contribution to Lung Infection, Inflammation and Repair with a Focus on Wheeze and Asthma in the Pediatric Population. EC Microbiology. 2014; 1: 4–14.
[32] Lee YK, Menezes JS, Umesaki Y, Mazmanian SK. Proinflammatory T-cell responses to gut microbiota promote experimental autoimmune encephalomyelitis. Proceedings of the National Academy of Sciences of the United States of America. 2011; 108 Suppl 1: 4615–4622.
[33] Flaherty S, Reynolds JM. TLR Function in Murine CD4(+) T Lymphocytes and Their Role in Inflammation. Methods in Molecular Biology. 2016; 1390: 215–227.